

The IACOB project: A grid-based automatic tool for the quantitative spectroscopic analysis of O-stars

S. Simón-Díaz^(1,2), N. Castro⁽³⁾, A. Herrero^(1,2), J. Puls⁽⁴⁾, M. García^(1,2), and C. Sabín-Sanjulián^(1,2)

⁽¹⁾Instituto de Astrofísica de Canarias, 38200 La Laguna, Tenerife, Spain.

⁽²⁾Departamento de Astrofísica, Universidad de La Laguna, 38205 La Laguna, Tenerife, Spain.

⁽³⁾Inst. of Astronomy & Astrophysics, National Obs. of Athens, 15236 Athens, Greece.

⁽⁴⁾Universitätssternwarte München, Scheinerstr. 1, 81679 München, Germany.

E-mail: `ssimon@iac.es`

Abstract. We present the IACOB grid-based automatic tool for the quantitative spectroscopic analysis of O-stars. The tool consists of an extensive grid of FASTWIND models, and a variety of programs implemented in IDL to handle the observations, perform the automatic analysis, and visualize the results. The tool provides a fast and objective way to determine the stellar parameters and the associated uncertainties of large samples of O-type stars within a reasonable computational time.

1. Introduction

The era of large spectroscopic surveys of massive stars has already begun, providing us with a huge amount of high-quality spectra of Galactic and extragalactic O-type stars. The *IACOB spectroscopic survey of Northern Galactic OB-stars* is one of them. This long-term observational project is aimed at building a multi-epoch, homogeneous spectroscopic database of high-resolution, high signal-to-noise ratio spectra of Galactic bright OB-stars¹. Associated with this spectroscopic dataset are several working packages aimed at its scientific exploitation. Within the framework of the Working Package *WP3: Quantitative Spectroscopic Analysis*, we have developed a powerful tool for the automatic analysis of optical spectra of O-type stars. The tool provides a fast and objective way to determine the stellar parameters and the associated uncertainties of large samples of O-stars within a reasonable computational time. Initially developed to be used for the analysis of spectra of O-type stars from the *IACOB spectroscopic database*, the tool is now also being applied in the context of the *VLT-FLAMES Tarantula Survey* (VFTS) project [3], and other studies of stars of this type.

2. The IACOB grid-based tool

Apart from the already mentioned characteristics (automatic, objective, and fast), we also aimed at a tool that is portable, versatile, adaptable, extensible, and easy to use. As shown throughout the following text, this philosophy has guided the whole development of the tool.

¹ Some notes on the present status of *IACOB spectroscopic database*, the IACOB project, and the various working packages can be found in [1] and [2].

One of the key-stones of any automatic quantitative spectroscopic analysis is the computation of large samples of synthetic spectra (using a stellar atmosphere code), to be compared with the observed spectrum. In contrast to other possible alternatives (the *genetic algorithm* –GA– employed by [4], or the *principal component analysis* –PCA– approach followed by [5]), we decided to base our automatic tool on an extensive, precomputed grid of stellar atmosphere models and a line-profile fitting technique (i.e., a grid-based approach²). This option was possible thanks to the fast performance of the FASTWIND code³, and the availability of a cluster of ~ 300 computers at the Instituto de Astrofísica de Canarias (IAC) connected through the CONDOR⁴ workload management system.

The grid is complemented by a variety of programs implemented in IDL, to handle the observations, perform the automatic analysis, and visualize the results. The IDL-package has been built in a modular way, allowing the user, e.g., to easily modify how the mean values and uncertainties of the considered parameters are computed, or which evolutionary tracks will be used to estimate the evolutionary masses.

2.1. The IACOB FASTWIND grid

In the following we outline the main characteristics of the FASTWIND grid used for the analysis of Galactic O-type stars that is presently incorporated within the IACOB grid-based tool.

Input stellar parameters considered in the FASTWIND models:

- **Effective temperature (T_{eff}) and gravity ($\log g$):** Table 1 indicates the ranges of T_{eff} and $\log g$ considered in the grid. Basically, the grid points were selected to cover the region of the $\log T_{\text{eff}} - \log g$ diagram where the O-type stars are located.
- **Helium abundance (ϵ_{He}) and microturbulence (ζ_t):** The grid includes six values of helium abundance — $\epsilon_{\text{He}} = N_{\text{He}}/(N_{\text{H}} + N_{\text{He}})$ —, indicated in Table 1. For all models, a microturbulence $\zeta_{t,\text{mod}} = 15 \text{ km s}^{-1}$ was adopted in the computation of the atmospheric structure, and four values of the microturbulence were considered in the formal solution.
- **Radius (R):** Computing a FASTWIND model requires an input value for the radius. This radius has to be close to the actual one (which will be derived in the final step of the analysis, and hence is not known from the beginning on). We assumed a radius for each ($T_{\text{eff}}, \log g$) pair following the calibration by [8]. The grid is hence divided in 20 regions in which a different radius is considered. For example, for the case of $\log g = 4.0$ and 3.5 dex, the radii range from 7 to 12 R_{\odot} and from 19 to 22 R_{\odot} , respectively.
- **Wind parameters (\dot{M} , v_{∞} , β):** As conventional for grid computations of stellar atmosphere models for the optical analysis of O-stars, the mass loss rate (\dot{M}) and terminal velocity (v_{∞}) of the wind have been compressed, together with the radius, into the wind strength parameter (or optical depth invariant), $Q = \dot{M}/(v_{\infty} R)^{1.5}$ (see [7]). Ten $\log Q$ -planes were considered for the grid. For each FASTWIND model, \dot{M} and v_{∞} need to be specified. First, a terminal velocity $v_{\infty} = 2.65 v_{\text{esc}}$ was adopted, following [9]; then a mass loss rate was computed for the given $\log Q$, v_{∞} , and R . Finally, the exponent of the velocity law, β , was assumed as a free parameter ranging from 0.8 to 1.8.

² A similar approach has been recently applied by [6] for the analysis of a sample of 12 low resolution spectra of B supergiants in NGC55.

³ Among the various available modern stellar atmosphere codes incorporating wind and line-blanketing effects, FASTWIND [7] is the fastest.

⁴ <http://www.cs.wisc.edu/condor/>

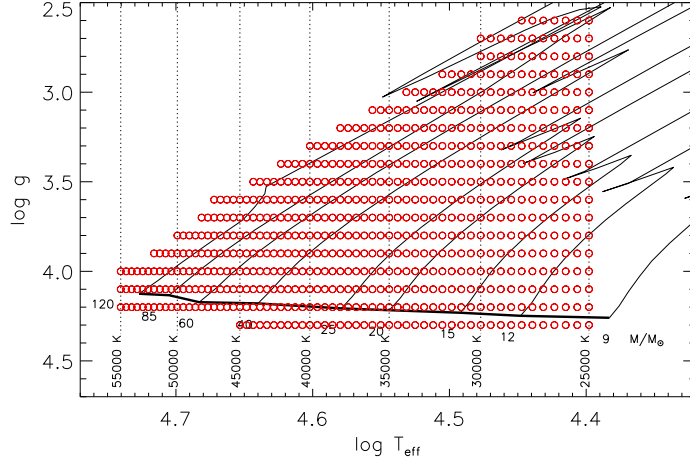


Figure 1. Location of $(T_{\text{eff}}, \log g)$ -pairs considered in the FASTWIND grid incorporated into the present version of the IACOB grid-based tool. Evolutionary tracks from [11].

Table 1. Range of values considered for the six free parameters in the FASTWIND grid.

$\log g$:	[2.6 – 4.3] dex (with step size 0.1 dex)
T_{eff} :	≥ 25000 K (step size 500 K), upper limit defined by the 120 M_{\odot} track (see Fig. 1)
ζ_t :	Model: 15 km s^{-1} , Formal solution: 5, 10, 15, 20 km s^{-1}
ϵ_{He} :	0.06, 0.09, 0.13, 0.17, 0.20, 0.23
$\log Q$:	-15.0, -14.0, -13.5, -13.0, -12.7, -12.5, -12.3, -12.1, -11.9, -11.7
β :	0.8, 1.0, 1.2, 1.5, 1.8

- **Metallicity:** A solar metallicity (following [10]) was assumed for the whole grid⁵.

Synthetic lines: The following (optical) lines were synthesized in the formal solution: $\text{H}_{\alpha-\epsilon}$, $\text{He I } \lambda\lambda 4026, 4120, 4143, 4387, 4471, 4713, 4922, 5015, 5048, 5875, 6678$, and $\text{He II } \lambda\lambda 4026, 4200, 4541, 4686, 5411, 6406, 6527, 6683$.

In order to optimize the size and the read-out time of the grid, only part of the output from the FASTWIND models is kept and stored in IDL xdr-files. This includes the input parameters, the H/He line profiles and equivalent widths, the information about the stellar atmosphere structure and the emergent flux distribution, and the synthetic photometry resulting from the computed emergent flux distribution. Using these xdr-files, the size of the grid can be reduced to a 10 % of the original one. IDL can restore each xdr-file and compute the corresponding X_T^2 quantity (see Sect. 2.2) in 0.02–0.1 s per model, i.e., the tool can pass through 80,000 models in 30 min–1 hour. Following the main philosophy of the IACOB grid-tool, only the reduced grid is used by the tool, whilst the original grid is safely kept on hard-disk at the IAC. This allows for an easy transfer of the grid to an external disk, hence satisfying our constraint for portability.

The FASTWIND grid presently incorporated into the IACOB grid-based tool consists of $\sim 192,000$ models ($\sim 32,000$ models per He-plane). The reduced size is ~ 34 Gb. This predefined grid can be easily updated and/or extended if necessary using appropriate scripts implemented in IDL, CONDOR, and LINUX. For example, a new He-plane can be computed and prepared for use in ~ 3 days.

⁵ We also calculated similar grids for other metallicities ($Z = 0.5, 0.4$, and $0.2 Z_{\odot}$).

2.2. The IACOB grid-based tool IDL package

The guideline of the automatic analysis is based on standard techniques applied within the quantitative spectroscopic analysis of O-stars using optical H/He lines that have been described elsewhere (e.g. [12], [13]). The whole spectroscopic analysis is performed by means of a variety of IDL programs following the steps indicated below. In brief, once the observed spectrum is processed, the tool obtains the quantity X_T^2 (i.e. an estimation of the goodness of fit) for each model within a subgrid of models selected from the global grid, and determines the stellar parameters and their associated uncertainties by interpreting the obtained X_T^2 distributions.

Step 1: The input

In this first step, the user has to provide the observed spectrum, to indicate the corresponding resolving power (R), and to give some pre-determined information about the star – the projected rotational velocity ($v \sin i$), the size of the extra line-broadening (Θ_{RF}), and the absolute visual magnitude (M_V).

Concerning the grid, the user must select the appropriate metallicity, and indicate the range of values for the various free parameters (defining the subgrid of models to be considered within the analysis). This latter option allows the tool to be faster (using optimized ranges for the various free parameters), or the user to perform a preliminary quick analysis by fixing some of the parameters. For example, one can obtain a quick estimate on T_{eff} , $\log g$, and $\log Q$ in less than 5 min, by fixing the other three parameters (ζ_t , ϵ_{He} , and/or β).

Finally, the H/He lines which shall be considered in the analysis and the corresponding weights need to be specified.

Step 2: Processing of the observed spectrum

In many cases, the observed spectra need to be processed before launching the automatic analysis, because of, e.g., nebular contamination affecting the cores of the H and He I lines, the need to improve the normalization of the continuum adjacent to the line, and the presence of cosmic rays.

The possibility to correct the observed spectrum for these effects has been incorporated into corresponding IDL procedures. The implemented options include (for each of the considered lines): local renormalization, selection of the wavelength range of the line, clipping/restoring of certain parts of the line, and computation of the signal-to-noise ratio (S/N) in the adjacent continuum.

Once finalized, the processed spectrum is stored. This spectrum and all associated information is used in *Step 3*, and also each time the analysis of the same star/spectrum is (re-)launched. This way the user can easily reconsider his/her decisions after a first analysis.

In this step, the user can select a model from the grid to help him/her with the processing of the observed spectrum. One can, for example, make a quick preliminary analysis (see above) fixing some parameters and including only few lines, and then use the resulting best model to check the processed lines and find constraints for the processing of the others.

Step 3: Estimation of the goodness of fit for each considered model

This step, together with *Step 4*, are the most important ones, constituting the core of the program. In the present version of the IACOB grid-based tool we have considered a procedure as described below; however, we are aware that this procedure can be subject to discussion/improvements. Having this in mind, and following the philosophy of the tool (regarding versatility and adaptability), the corresponding IDL modules have been implemented with the

possibility to be easily modified. The fast performance of the IACOB grid-based tool makes it very powerful to investigate various alternative strategies.

In our present version, the tool computes, for every model in the subgrid, the quantity X_L^2 for each considered line

$$X_L^2 = \frac{1}{N_\lambda} \sum_{\lambda=1}^{N_\lambda} \frac{(F_{m,\lambda} - F_{o,\lambda})^2}{\sigma_L^2} \quad (1)$$

where $F_{m,\lambda}$ and $F_{o,\lambda}$ are the normalized fluxes corresponding to the synthetic and observed spectrum, respectively; $\sigma_L = (\text{S/N})^{-1}$ accounts for the S/N of the line; and N_λ is the number of frequency points in the line. Under ideal conditions (e.g., for a perfect model, but see below), X_L^2 corresponds to a reduced χ^2 .

In a second step, the X_L^2 values for each model are corrected for possible deficiencies in the synthetic lines (due, for example, to deficiencies in the model, an incorrect characterization of the noise of the line, bad placement of the continuum, or bad characterization of the line-broadening). To this aim we compute, for each line, the standard deviation of the residuals $\sigma_c = \sigma(F_{m,\lambda} - F_{o,\lambda})$ from that model that results in the minimum X_L^2 for the given line. Then, the following correction is applied:

$$X_{L,c}^2 = X_L^2 \frac{\sigma_L^2}{\sigma_c^2} \quad (2)$$

Using these individual $X_{L,c}^2$ values and the weights assumed for each of the considered lines (w_L , e.g., [4]), a global X_T^2 is obtained:

$$X_T^2 = \sum_{L=1}^{N_L} w_L X_{L,c}^2 \quad (3)$$

where N_L is the number of lines. For a large number of frequency points per line, X_T^2 should be normally distributed.

Thus, *Step 3* provides the values of the quantity X_T^2 associated with each of the models included in the considered subgrid. As indicated in Section 2.1, this step can last from a few seconds to less than about 1 hour, depending on the number of models in the subgrid. An example of X_T^2 -distributions (actually, $p_{X_T^2} = e^{-0.5X_T^2}$) with respect to the various stellar parameters is presented in Figure 2.

Step 4: Computation of mean values and uncertainties

The previous step provides the X_T^2 -distributions for each of the six parameters derived through the spectroscopic analysis (T_{eff} , $\log g$, ϵ_{He} , ζ_t , $\log Q$, and β). If the absolute visual magnitude is provided, the tool automatically determines R , $\log L$, and M_{sp} (spectroscopic mass) for each model, and hence the corresponding X_T^2 -distributions for these parameters are available as well. If also the terminal velocity is provided, a similar computation is performed for the mass-loss rate (using Q , R , and v_∞). Finally, one of the IDL modules computes the evolutionary masses (M_{ev}) of the models from an interpolation in the $(\log T_{\text{eff}}, \log g)$ -plane using the tracks provided by a stellar evolution code. Since the X_T^2 -distributions for T_{eff} and $\log g$ are computed and stored in *Step 3*, the computation of the corresponding distributions for R , $\log L$, M_{sp} , M_{ev} can be easily repeated in a few seconds, in case a different M_v and/or evolutionary tracks need to be considered.

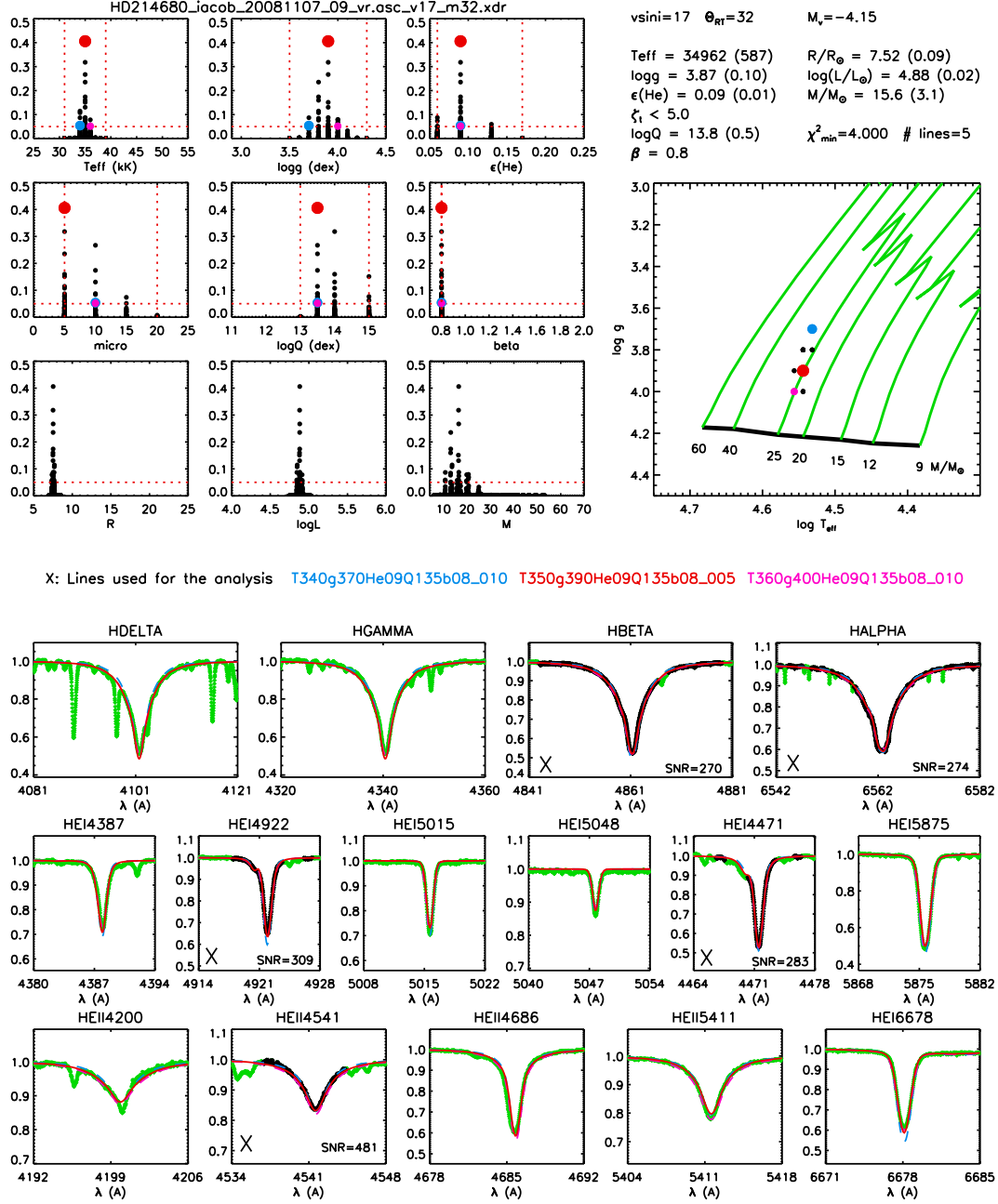


Figure 2. Example of output provided by the IACOB grid-based tool, for the quantitative spectroscopic analysis of the Galactic O9 V star HD 214680. See text for the explanation of all the information contained in the figure. Observed spectrum from the *IACOB spectroscopic database* ($R=46,000$). $v \sin i$ and Θ_{RT} were previously determined using a combined Fourier transform + goodness of fit technique (see e.g. [14]). In this example, only 5 H/He lines were used for the actual analysis. Note that also all other synthetic lines fit the observations perfectly at the derived parameters. The analysis was performed in ~ 2 min. See [2] for details on the distance, apparent visual magnitude and visual extinction used to determine the absolute visual magnitude (M_v).

These distributions are then used to compute mean values and uncertainties for each parameter (taking into account that models above a given threshold in X_T^2 can be discarded).

The tool also allows to easily investigate possible degeneracies (for example, for stars with weak winds the analysis of the optical H/He lines only provides an upper limit for the Q parameter, and does not allow to constrain β), and the contribution of the various parameters to the final uncertainty (by fixing one of the free parameters to a certain value and recomputing the statistics for the other parameters).

Step 5: Visualization of the results

The last step is the creation of a summary plot for better visualization of the results (see Figure 2 as an example). The present version of the tool includes:

- $p_{X_T^2}$ – distributions for the various parameters involved in the analysis (upper-left panels). In those panels, vertical lines indicate the limiting values adopted for the six free parameters (i.e., the sub-grid of FASTWIND models for which a X_T^2 is computed), and horizontal lines indicate the $p_{X_T^2}$ value corresponding to $X_T^2(\text{threshold})$. The user can select three of the models that will be indicated as red, blue, and pink dots (the same colors are also used in other parts of the figure).
- a summary of the input parameters ($v \sin i$, Θ_{RT} , and M_V) and the result from the statistics for each parameter resulting from the analysis (upper-right part of the figure).
- a $\log T_{\text{eff}} - \log g$ diagram including evolutionary tracks (e.g., from [11], without rotation, in the figure) and the position of all models with $X_T^2 \leq X_T^2(\text{threshold})$.
- a set of panels (lower part of the figure) where the observed and synthetic H/He lines indicated by the user are compared. The spectral regions that are used to compute the X_T^2 for each line are indicated in black, while the clipped (or not used) regions are presented in green. Note that the plotted lines are not limited to those used in the analysis process (the latter are marked with an 'X').

2.3. Problems that can be investigated with the IACOB grid-based tool

The fast performance and versatility of the IACOB grid-based tool not only allows to analyze large samples of O-type stars in a reasonable time, but also to easily investigate the effects of

- *the assumed line-broadening*: The common strategy in previous spectroscopic analyses of O-stars was to assume pure rotational line-broadening (in addition to natural, thermal, Stark/collisional and microturbulent broadening included in the synthetic spectra). However, recent studies have shown that an important extra-broadening contribution (commonly quoted as *macroturbulent broadening*) affects the shape of the line-profiles of this type of stars (see e.g. [15], and references therein). How much are the derived parameters affected when this extra-broadening is neglected? Can both broadening contributions be represented by one 'fake' rotational profile ($v_f \sin i$), without disturbing the resulting parameters? What is the effect of the uncertainty in the derived/assumed broadening? Some results from a preliminary investigation of these questions can be found in [16].
- *the placement of the continuum*: The normalization of the spectra of O-type stars is sometimes complicated, especially in the case of echelle spectra. It is commonly argued that the derived gravity can be severely affected by the assumed normalization, but, to which extent? To investigate this effect one could use the IACOB grid-based tool, applying small modifications to the continuum placement. An example of this type of analysis for the case of low resolution spectra of B-supergiants can be found in [6].

- *neglecting/including a variety of different commonly used diagnostic lines*: Before computing the global X_T^2 (see equation 3), the resulting X_L^2 for each line are stored. This way the user can easily recompute X_T^2 , discarding some of the initially considered lines. This option allows, for example, to investigate the change in the wind-strength parameter when both H α and He II 4686 lines or only one of them are included in the analysis.
- *clipping part of the lines*: Most of the O-stars are associated to H II regions. In some cases, the stellar spectra can be heavily contaminated by nebular emission lines (mainly the cores of the hydrogen lines, but also the He I lines). This contamination must be identified and eliminated from the stellar spectrum to obtain meaningful results from the spectroscopic analysis. When the resolution of the spectra is high, the clipped region is small in comparison with the total line width; however, even for a moderate resolution an important region of the line needs to be eliminated. What is the effect of such a strong clipping in the H α line on the determination of the mass-loss rate? How large is the effect of clipping the core of the He I lines in the T_{eff} determination?
- *the way the statistics is derived from the X_T^2 – distributions*: As commented in Section 2.2, this is a critical point in the determination of final best values and uncertainties.

These are only some examples of things can be investigated with the IACOB grid-based tool. Many other tests can be easily performed. In addition, we expect the tool to be of great benefit for the analysis of the O-star samples included in, e.g., the ESO-Gaia, VFTS, OWN, IACOB and other similar large surveys.

Acknowledgments

Financial support by the Spanish Ministerio de Ciencia e Innovación under projects AYA2008-06166-C03-01, AYA2010-21697-C05-04, and by the Gobierno de Canarias under project PID2010119. This work has also been partially funded by the Spanish MICINN under the Consolider-Ingenio 2010 Program grant CSD2006-00070: First Science with the GTC (<http://www.iac.es/consolider-ingenio-gtc>).

References

- [1] Simón-Díaz S, Castro N, García M, Herrero A and Markova N 2011a, *BRSR Liege*, **80**, 514
- [2] Simón-Díaz S, García M, Herrero A, Maíz-Apellániz J, and Negueruela I 2011b, *Proc. Conf. "Star clusters and Associations: A RIA Workshop on Gaia"* Preprint arXiv1109.2665S
- [3] Evans C J et al. 2011, *A&A*, **530**, A108
- [4] Mokień M R, de Koter A, Puls J, Herrero A, Najarro F and Villamariz M R 2005, *A&A*, **441**, 711
- [5] Urbaneja M A, Kudritzki R P, Bresolin F, Przybilla N, Gieren W and Pietrzyński G 2008, *ApJ*, **684**, 118
- [6] Castro, N., Herrero, A., Urbaneja, M. A, et al. (*A&A*, submitted)
- [7] Puls J, Urbaneja M A, Venero R, Repolust T, Springmann U, Jokuthy A and Mokień M R 2005, *A&A*, **435**, 669
- [8] Martins F, Schaerer D and Hillier, D. J. 2005, *A&A*, **436**, 1049
- [9] Kudritzki R P and Puls J 2000, *A&A*, **38**, 613
- [10] Asplund M, Grevesse N, Sauval A J and Scott P 2009, *ARA&A*, **47**, 481
- [11] Schaller G, Schaerer D, Meynet G and Maeder A 1992, *A&AS*, **96**, 269
- [12] Herrero A, Puls J. and Najarro F 2002, *A&A*, **396**, 949
- [13] Repolust T, Puls J and Herrero A 2004, *A&A*, **415**, 349
- [14] Simón-Díaz S, Herrero A, Uytterhoeven K, Castro N, Aerts C and Puls J 2010, *ApJL*, **720**, L174
- [15] Simón-Díaz S 2011, *BRSR Liege*, **80**, 86
- [16] Sabín-Sanjuan C, Simón-Díaz S, García M, Herrero A, Puls J and Castro N 2011, *Proc. Conf. in Honour of A. Moffat*